NUMERICAL EVALUATION OF NON-INFRARED TWO-LOOP VERTICES* **

Sandro Uccirati

Max-Planck-Institut für Physik, Werner-Heisenberg-Institut
Föhringer Ring 6, 80805 München, Germany
e-mail: uccirati@mppmu.mpg.de

Some methods for the numerical computation of two-loop non-infrared vertices are reviewed. A new method is also proposed and compared to the old ones. Finally, some preliminary results are presented, concerning the evaluation of the fermionic corrections to $\sin^2 \theta_{\mathrm{eff}}^{\mathrm{lept}}$ through the described techniques.

PACS numbers: 12.15.Lk, 02.60.Jh

1. Introduction

In the forthcoming experiments, the validity of the Standard Model will be tested with high precision. In addition to the direct search of the Higgs Boson, important quantities will be measured in the future colliders, providing a good test of the Model. This of course pushes the theorists to compute these observables at the same degree of precision. For example, the mass of the W boson, whose present value is $M_W = 80.426 \pm 0.034$ GeV ([1]), will be measured with an expected error of 15 MeV at LHC and 6 MeV at the ILC. Or the effective leptonic weak mixing angle ($\sin^2 \theta_{\mathrm{eff}}^{\mathrm{lept}} = 0.23150(16)$, [1]) will be known with an absolute precision of 10^{-5} at the ILC. To get a similar theoretical uncertainty, we have to improve the calculation in perturbation theory beyond the one-loop level. The computation of two-loop Feynman diagrams is a hard task. The pure analytical techniques are very efficient when few mass scales are present (see for example [2] or [3]), but seem to be unable to deal with the complete set of two-loop diagrams in the Standard

---

Model (where more scales come into the game). For this reason we were led to abandon the analytical way in favour of a numerical evaluation of multi-loop diagrams. The goal of the numerical approach is to express any diagram in terms of smooth integrals.

2. Standard BT relation

The Bernstein–Tkachov theorem [4] tells us that for any finite set of polynomials $V_i(x)$, where $x = (x_1, \ldots, x_N)$ is a vector of Feynman parameters, there exists an identity of the following type:

$$\mathcal{F}(x, \partial) \prod_i V_i^{\mu_i + 1}(x) = B \prod_i V_i^{\mu_i}(x), \tag{1}$$

where $\mathcal{F}$ is a polynomial of x and $\partial_i = \partial/\partial x_i$; B and all coefficients of $\mathcal{F}$ are polynomials of μ_i and of the coefficients of $V_i(x)$. If the polynomial V is of second degree we have a master formula, again due to Tkachov [4]. We write the quadratic V as:

$$V(x) = x^t H x + 2 K^t x + L, \tag{2}$$

where $x^t = (x_1, ..., x_n)$, H is an $n \times n$ matrix, K is an n vector. The solution to the problem of determining the polynomial $\mathcal{F}$ is as follows:

$$\mathcal{F} = 1 + \frac{\mathcal{P}^t \partial_x}{\mu + 1}, \qquad \mathcal{P} = -\frac{x - X}{2}, \tag{3}$$

$$B = L - K^t H^{-1} K, \qquad X = -H^{-1} K. \tag{4}$$

Therefore we have:

$$V^\mu(x) = \frac{1}{B} \left[1 + \frac{\mathcal{P}^t \partial_x}{\mu + 1} \right] V^{\mu+1}(x). \tag{5}$$

This is the standard BT relation for quadratics.

3. Strategy

The standard BT relation is very useful for the computation of one-loop diagrams and also some two-loop configurations (see [5–9]). The strategy is the following. First of all, the diagram with N external legs and a tensorial structure of rank n is decomposed in form factors:

$$G_N^{\mu_1, \ldots, \mu_n} = \sum_T G_N(T) T^{\mu_1, \ldots, \mu_n}. \tag{6}$$

Here $T^{\mu_1,\dots,\mu_n}$ are all possible tensors of rank n that can be obtained by combining the $N-1$ independent external momenta of the diagram and the metric $\delta_{\mu\nu}$.

For one-loop diagrams, if we write each form factor in the parametric space, we always obtain a result of this form (see [7] for details):

$$G_N = \left(\frac{\mu^2}{\pi}\right)^{\varepsilon/2} \Gamma\left(n+\frac{\varepsilon}{2}\right) \int dS_{N-1}(x), , P(x)\, V(x)^{-n-\varepsilon/2} \qquad n \in \mathbb{N}, \quad (7)$$

where

$$\int dS_m(z) = \int\limits_0^1 dz_1 \int\limits_0^{z_1} dx_2 \dots \int\limits_0^{z_{m-1}} dz_m \,, \qquad (8)$$

μ is the mass scale and P and V are polynomials in the Feynman parameters $x = (x_1,\dots,x_{N-1})$. In particular $V(x)$ is always a quadratic of the type Eq. (2). The Γ function contains the UV pole (if present) of the diagram. Its argument is always equal to the exponent of V with opposite sign and therefore, for every UV divergent one-loop diagram, V has a vanishing power.

The goal is to express G_N in terms of smooth integrals to be integrated numerically. For $n = 0$ (which corresponds to UV divergent form factors), we can simply perform a Laurent expansion around $\varepsilon = 0$ to get just smooth integrands of the type:

$$P(x)\, \ln^k V(x)\,. \qquad (9)$$

For $n \geq 1$ the idea is to apply the BT relations Eq. (5) to "raise" the power of V of one unit and then integrate by parts to get rid of the derivatives. Then the procedure is repeated for all integrals that are generated, until the power of V becomes $-\varepsilon/2$, and, at this point, we proceed as in the case $n = 0$.

The procedure is clear and leads to smooth integrals at the price of introducing the denominator B which of course can vanish somewhere in the phase space. It can be proved that the zeros of B correspond to the leading Landau singularity of the diagram, but the singular behaviour is usually overestimated by the BT procedure (see [7]). This means that in the region $B \sim 0$ all terms generated by Eq. (5) cancel one another, giving rise to numerical instabilities. For this reason it would be good to find a new relation, which should contain the real divergent behaviour for $B = 0$ and therefore should remain stable also for $B \sim 0$.

In the two-loop case the form factors are classified counting the number of propagator of each loop:

$$G_N(T) \quad \to \quad G_{abc}(T), \qquad (10)$$

where a is the number of propagators (with momentum q_1) which belong just to the first loop (the one with the smallest number of propagators), b is the number of propagators (with momentum q_2) which belong just to the second loop and c is the number of propagators (with momentum $q_1 - q_2$) which belong to both loops.

Then we first parametrise the loop with momentum q_1, obtaining a new propagator in q_2 with a non integer power. The mass and the momentum of this new propagator depend in general on the Feynam parameters of the first loop. After the parametrisation of the second loop, each form factor takes the form (see [10] for details):

$$
\begin{aligned}
G_{abc} = \; & \mathcal{A}_\varepsilon \left(\frac{\mu^2}{\pi} \right)^\varepsilon \Gamma\left(n + \varepsilon \right) \int dS_{a+c-1}(x) \int dS_b(x) \\
& \times [x_2 \left(1 - x_2 \right)]^{-m-\varepsilon/2} \, y_b^{m-1+\varepsilon/2} P(x,y) \, V_x(y)^{-n-\varepsilon} \,, \qquad (11)
\end{aligned}
$$

where $m, n \in \mathbb{N}$, μ is again the mass scale and $\mathcal{A}_\varepsilon$ is a constant regular in $\varepsilon = 0$. P is a polynomial in all Feynman parameters $x = (x_1, \ldots, x_{a+c-1})$ and $y = (y_1, \ldots, y_b)$. $V_x(y)$ is a quadratic of the type Eq. (2) in y, where now the coefficients H, K, L depend on x and have the following form:

$$
\frac{C(x)}{x_2^h \left(1 - x_2 \right)^k} \,, \qquad (12)
$$

where $h, k \in \mathbb{N}$ and C is quadratic in x. The Γ function contains the overall UV pole (if present), while sub-divergencies are contained in $[x_2(1 - x_2)]^{-m-\varepsilon/2} y_b^{m-1+\varepsilon/2}$. Since at least one of the coefficients of V_x have in the denominator the product $x_2 \left(1 - x_2 \right)$, the divergent behaviour of the integrand at $x_2 = 0$ and $x_2 = 1$ is present (generating the UV pole) just for $m > n$. On the other hand the UV divergency is generated by the behaviour in $y_b = 0$ only for $m = 0$.

So, apart the UV pole coming from sub-loops, any two-loop diagram is the integral of a one-loop diagram whose masses and momenta depend on the integration variables. If we would be able to express any one-loop diagram in terms of smooth integrals not only with respect to the integration variables, but also with respect to their external masses and momenta, the numerical evaluation of two-loop diagrams would be a trivial task. The BT relation Eq. (5) is in general not good for this purpose, because it introduces the denominator B. In fact, since the coefficients H, K and L of V_x (Eq. (11)) depend on the Feynman variables x, the same happens for B which therefore generates singularities inside the x integration contour. As a consequence, apart some special cases where it is possible to have a factor B independent of any Feynman variable, the standard BT method cannot be applied for

two-loop diagrams. This is another reason to search for a new BT-like relation.

4. The new BT-like relation

To obtain new relations it is useful to write the quadratic $V(x)$ in the following way:

$$
\begin{aligned}
V(x) &= x^t\,H\,x + 2\,K^t\,x + L \\
&= (x^t - X^t)\,H\,(x - X) + B = Q(x) + B\,.
\end{aligned}
\tag{13}
$$

This formula, which defines the quadratic $Q(x)$, can be trivially verified using the definition of B and X in Eq. (4). The basic relation satisfied by $Q(x)$ is the following:

$$
\mathcal{P}^t\,\partial_x\,Q(x) = -Q(x)\,, \qquad \mathcal{P} = -\frac{x - X}{2}\,.
\tag{14}
$$

At this point we introduce a new variable y and a new polynomial $W(x,y)$ defined as follows:

$$
W(x,y) = Q(x)\,y + B\,,
\tag{15}
$$

and satisfying the following relation:

$$
(\mathcal{P}^t\,\partial_x + y\,\partial_y)\,W^\mu(x,y) = 0\,.
\tag{16}
$$

Next we consider the following integral

$$
I_\beta = \int_0^1 dy\,y^{\beta-1}\,W^\mu(x,y)\,, \qquad \beta > 0
\tag{17}
$$

and compute:

$$
\mathcal{P}^t\,\partial_x\,I_\beta = \int_0^1 dy\,y^{\beta-1}\,\mathcal{P}^t\,\partial_x\,W^\mu(x,y) = -\int_0^1 dy\,y^{\beta}\,\partial_y\,W^\mu(x,y)
$$

$$
= -W^\mu(x,1) + \beta \int_0^1 dy\,y^{\beta-1}\,W^\mu(x,y) = -V^\mu(x) + \beta\,I_\beta.
\tag{18}
$$

Using the definition of the hypergeometric function (see [11]) to evaluate I_β, we finally get:

$$
V^\mu(x) = B^\mu\left(1 - \frac{\mathcal{P}^t\,\partial_x}{\beta}\right){}_2F_1\left(-\mu\,,\,\beta\,;\,\beta+1\,;\,-\frac{Q}{B}\right).
\tag{19}
$$

This formula has a general validity and does not depend on the actual expression for Q, B and $\mathcal{P}$. The only relations which they must satisfy are:

$$V(x) = Q(x) + B, \qquad \mathcal{P}^t \, \partial_x \, Q(x) = -Q(x), \qquad \beta > 0. \qquad (20)$$

The usefulness of this relation is evident if we consider the case $\mu = -1-\alpha\,\varepsilon$. In this case the better choice for the free parameter β is $\beta = 1$. Using the expansion of the hypergeometric function around $\varepsilon = 0$

$$\,_2F_1\left(1 + \alpha\,\varepsilon\,,\, 1\,;\, 2\,;\, x\right) = -\frac{1}{x} \sum_{n=0}^{\infty} \frac{(-\alpha\,\varepsilon)^n}{(n+1)!} \, \ln^{n+1}(1-x), \qquad (21)$$

we obtain

$$V^{-1-\alpha\,\varepsilon} = \sum_{n=1}^{\infty} \frac{(-\alpha\,\varepsilon)^{n-1}}{n!} \left(1 - \mathcal{P}^t\,\partial_x\right) \frac{B^{-\alpha\,\varepsilon}}{Q} \, \ln^n\left(1 + \frac{Q}{B}\right). \qquad (22)$$

In this relation we have obtained our goal to avoid the appearance of the factor B in the denominator. Here, the only denominator is $Q(x)$ which can vanish inside the integration contour; however its zeros are compensated by the logarithm, whose argument goes to 1 when $Q(x)$ goes to 0.

An example of the usefulness of the new relation is the evaluation of one-loop three-point functions. In the scalar case we have:

$$C_0 = \left(\frac{\mu^2}{\pi}\right)^{\varepsilon/2} \Gamma\left(1 + \frac{\varepsilon}{2}\right) \int_0^1 dx_1 \int_0^{x_1} dx_2 \, V(x_1, x_2)^{-1-\varepsilon/2}. \qquad (23)$$

If we insert Eq. (22) and integrate by parts, we simply obtain:

$$C_0 = \sum_{i=0}^{2} \frac{a_i}{2} \int_0^1 dx \, \frac{1}{Q[i](x)} \, \ln\left(1 + \frac{Q[i](x)}{B}\right) + \mathcal{O}(\varepsilon), \qquad (24)$$

where

$$\begin{aligned} Q[0](x) &= Q(1, x)\,, & Q[1](x) &= Q(x, x)\,, & Q[2](x) &= Q(x, 0)\,, (25) \\ a_0 &= 1 - X_1\,, & a_1 &= X_1 - X_2\,, & a_2 &= X_2\,. & (26) \end{aligned}$$

This result for C_0 (which can be easily generalised for tensor integrals) can be also used to compute two-loop diagrams which can be expressed as an integral of a one-loop three-point function. We see for example what happens in two families of two-loop vertices.

5. The two-loop vertex V^{131}

All two-loop vertices can be classified according to six families. Their list is given in the Appendix. Taking into consideration the V^{131} vertex, after Feynman parametrisation it takes the form:

$$V^{131} = -\left(\frac{\mu^2}{\pi}\right)^\varepsilon \Gamma\left(1+\varepsilon\right) \int_0^1 dx \int dS_3(y,z_1,z_2)\,[x(1-x)]^{-\varepsilon/2}(1-y)^{\varepsilon/2-1}\,U^{-1-\varepsilon},$$
(27)

$$U = (z^t - X^t)\,H\,(z-X) + (m_x^2 - m_3^2)\,(1-y) + B, \qquad m_x^2 = \frac{m_1^2}{x} + \frac{m_2^2}{1-x}, \quad (28)$$

where the masses are defined in the figure for V^{131} in the Appendix. The coefficient H, X and B are those appearing in the polynomial of a one-loop three-point function, with external momenta $-P$, p_1, p_2 and masses m_3, m_4, m_5. If we introduce $Q(y,z_1,z_2)$ for the polynomial U defined by:

$$U(y,z_1,z_2) = Q(y,z_1,z_2) + B,$$
(29)

we see that Q satisfies the following basic relation:

$$\left[(1-y)\,\partial_y - \frac{(z^t - X^t)\,\partial_z}{2}\right] Q = -Q.$$
(30)

From this formula we obtain the standard BT relation and the new one (choosing $\beta = 1$):

$$U^{-1-\varepsilon} = \frac{1}{B}\left[1 - \frac{(1-y)\,\partial_y}{\varepsilon} + \frac{(z^t - X^t)\,\partial_z}{2\,\varepsilon}\right] U^{-\varepsilon},$$
(31)

$$U^{-1-\varepsilon} = \sum_{n=1}^\infty \frac{(-\varepsilon)^{n-1}}{n!}\left[1 - (1-y)\partial_y + \frac{(z^t - X^t)\partial_z}{2}\right]\frac{B^{-\varepsilon}}{Q}\ln^n\left(1 + \frac{Q}{B}\right).$$
(32)

From these equations, we see that V^{131} is exactly one of those particular two-loop configurations for which a factor B independent of any Feynman parameter can be found. If this is crucial for the application of the standard BT method (Eq. (31)), this would not be strictly required for the new method (Eq. (32)). In addition to that the new relation appears to have a better behaviour near the zeros of B.

However, for this type of diagrams, where the polynomial U is linear in one of the Feynman variables (y), another procedure is available. After the

transformation $y \to 1 - (1 - z_1)\, y$, we have to compute:

$$I = \int_0^1 dy\, y^{\varepsilon/2-1} \left(a\, y + b\right)^{-1-\varepsilon} = \frac{2\, b^{-1-\varepsilon}}{\varepsilon}\, {}_2F_1\left(1 + \varepsilon\,,\, \frac{\varepsilon}{2}\,;\, \frac{\varepsilon}{2} + 1\,;\, -\frac{a}{b}\right),\quad (33)$$

$$a = \left(m_x^2 - m_3^2\right)(1 - z_1)\,, \qquad b = \left(z^t - X^t\right)H\left(z - X\right) + B\,. \qquad (34)$$

By applying the properties of the hypergeometric function (see [9] for details)

s	p_1^2	p_2^2	m_1	m_2	m_3	m_4	m_5	Re V_0^{131}
100^2	m_b^2	m_b^2	m_W	m_W	m_Z	m_b	m_Z	$0.274717(2) \times 10^{-2}$ $0.2747182(5) \times 10^{-2}$ 0.2747194×10^{-2}
800^2	m_b^2	m_b^2	m_W	m_W	m_Z	m_b	m_Z	$-0.247(4) \times 10^{-3}$ $-0.2456(9) \times 10^{-3}$ $-0.24612(8) \times 10^{-3}$
500^2	m_t^2	m_t^2	m_W	m_W	m_Z	m_t	m_Z	$0.952(1) \times 10^{-5}$ $0.9536(7) \times 10^{-5}$ $0.9545(13) \times 10^{-5}$
m_Z^2	m_e^2	m_e^2	m_t	m_t	m_Z	m_e	m_Z	$0.288416(3) \times 10^{-2}$ $0.288418(3) \times 10^{-2}$ 0.2884222×10^{-2}
m_Z^2	m_e^2	m_e^2	m_t	m_t	0	m_e	0	unstable $-0.195(47)$ $-0.214261(7)$
m_Z^2	m_e^2	m_e^2	m_e	m_e	0	m_e	0	unstable $0.2080(3)$ unstable

Fig. 1. Numerical results for the V^{131} family: $V^{131} = V_{-1}^{131}\, \varepsilon^{-1} + V_0^{131}$. All momenta are given in GeV. The first entry refers to the standard BT method Eq. (31), the second to the new method Eq. (32) and the third to Eq. (35). When no number appears in curly brackets, this means that the error does not affect the written digits. In the last two cases we have $B \sim 0$ and in the last case also $m_x^2 - m_3^2 \sim 0$.

and expanding in ε we simply obtain:

$$V^{131} = \int\limits_0^1 dz_1 \int\limits_0^{z_1} dz_2 \frac{1}{V} \ln\left(1 + \frac{V}{(m_x^2 - m_3^2)(1 - z_1)}\right)$$

$$+ \left(-\frac{2}{\varepsilon} + \int\limits_0^1 dx \ln A_x\right) C_0(P^2, p_1^2, p_2^2, m_3, m_4, m_5), \qquad (35)$$

where

$$V = (z^t - X^t) H (z - X) + B, \qquad A_x = -m_3^2 x (1-x) + m_1^2 (1-x) + m_2^2 x. \qquad (36)$$

Note that V is exactly the polynomial of the C_0 function appearing in Eq. (35). The numerical results for the three methods are then compared in Fig. 1.

6. The two-loop vertex V^{231}

Another important example of two-loop vertex topologies is V^{231} (see Appendix). In this case Feynman parametrisation gives:

$$V^{231} = -\left(\frac{\mu^2}{\pi}\right)^\varepsilon \Gamma(2 + \varepsilon) \int dS_2(x_1, x_2) [x_2(1 - x_2)]^{-1-\varepsilon/2}$$

$$\times \int dS_3(y_1, y_2, y_3) y_3^{\varepsilon/2} U^{-2-\varepsilon}, \qquad (37)$$

where

$$U = -[p_2 y_1 - P(y_2 - \mathcal{X} y_3) + p_1]^2 + (P^2 - p_1^2 + m_6^2 - m_5^2) y_1$$
$$- (P^2 + m_6^2 - m_4^2) y_2 + (M_x^2 - m_4^2) y_3 + p_1^2 + m_5^2, \qquad (38)$$

$$\mathcal{X} = \frac{1 - x_1}{1 - x_2}, \qquad M_x^2 = \frac{-P^2 x_1^2 + x_1 (P^2 + m_1^2 - m_2^2) + x_2 (m_3^2 - m_1^2) + m_2^2}{x_2 (1 - x_2)}. \qquad (39)$$

Now the polynomial U is a quadratic in y_1, y_2 and y_3 of the type $U = y^t H y + 2 K^t y + L$ and in principle we could apply the new BT-like relation for $\mu = -2 - \varepsilon$. Nevertheless, this would not be the most clever approach, because in this case the H matrix is singular and therefore the BT-factors B and X are not well-defined. Anyway, thanks to this singularity, we can perform the following change of variable

$$y_2 \to y_2 + \mathcal{X} y_3 \qquad (40)$$

and obtain a new polynomial U' which is now linear in y_3. Since this diagram is not UV divergent, we can set $\varepsilon = 0$ and the integration in y_3 becomes trivial, giving:

$$
V^{231} = \int dS_2(x_1, x_2) \int\limits_0^1 dy_1 \frac{1}{A(x)}
$$

$$
\times \left\{ \int\limits_{(1-\mathcal{X})y_1}^{y_1} dy_2 \left[\frac{x_2(1-x_1)}{(y_1-y_2)A(x) + x_2(1-x_1)B(y)} - \frac{1}{B(y)} \right] \right.
$$

$$
\left. + \int\limits_0^{(1-\mathcal{X})y_1} dy_2 \left[\frac{x_2(x_1-x_2)}{y_2 A(x) + x_2(x_1-x_2)B(y)} - \frac{1}{B(y)} \right] \right\}, \qquad (41)
$$

where $A(x)$ and $B(y)$ are quadratics, respectively in x_1, x_2 and y_1, y_2. Therefore each term is now a quadratic in y_1, y_2 to power -1 with x-dependent coefficients. In other words, the y-integrations are one-loop 3-point functions C_0 with x-dependent masses and momenta (of course some change of variable has to be done to reduce to the usual simplex in y_1, y_2). Note that

$s, -p_1^2, -p_2^2$	$m_1, m_2, m_3, m_4, m_5, m_6$	Re V^{231}
$100^2, m_b^2, m_b^2$	$m_b, m_b, m_z, m_b, m_z, m_b$	$0.5028(4) \times 10^{-7}$
$200^2, m_b^2, m_b^2$	$m_b, m_b, m_z, m_b, m_z, m_b$	$0.9816(20) \times 10^{-8}$
$8m_t^2, m_t^2, m_t^2$	$m_t, m_t, m_z, m_t, m_z, m_t$	$0.1489(5) \times 10^{-8}$
$20m_t^2, m_t^2, m_t^2$	$m_t, m_t, m_z, m_t, m_z, m_t$	$0.1675(6) \times 10^{-8}$
m_z^2, m_e^2, m_e^2	$m_t, m_t, m_t, m_z, m_e, m_z$	$-0.2018966 \times 10^{-8}$
m_z^2, m_e^2, m_e^2	$m_t, m_t, m_t, 0, m_e, 0$	$0.5987(6) \times 10^{-6}$
m_z^2, m_e^2, m_e^2	$m_e, m_e, m_e, 0, m_e, 0$	$-0.21161(49) \times 10^{-3}$

Fig. 2. Numerical results for the V^{231} family. All momenta are given in GeV. When no number appears in curly brackets, this means that the error does not affect the written digits.

the zeros of $A(x)$ do not spoil the smoothness of the integrand because the C functions cancel one another in the limit $A(x) \to 0$. At the end the diagram is written in the following form

$$V^{231} = \int dS_2(x_1, x_2) \, \frac{1}{A(x)} \left[C_0^{(1)} - C_0^{(2)} + C_0^{(3)} - C_0^{(4)} \right] \qquad (42)$$

and computed numerically using for the C_0 functions the expression of Eq. (24) obtained with the new method. The numerical results are shown in Fig. 2.

7. Work in progress: fermionic correction to $\sin^2 \theta_{\text{eff}}^{\text{lept}}$

The effective leptonic weak mixing angle is at present the observable that can give the most stringent indirect evaluation on the mass of the Higgs boson (by means of the radiative corrections). In the future, if the Higgs boson would be discovered, $\sin^2 \theta_{\text{eff}}^{\text{lept}}$ would represent a strong test of the Standard Model. It is defined through the vectorial and axial effective couplings g_v and g_a of the Z boson with leptons:

$$\sin^2 \theta_{\text{eff}}^l = \frac{1}{4} \left(1 - \text{Re} \left(\frac{g_v}{g_a} \right) \right). \qquad (43)$$

The effective couplings g_v and g_a are defined through the amplitude of the decay of an on-shell Z boson into two leptons:

$$\mathcal{M}_{Zll}^l = \bar{u}_l \, \mathcal{M}^\mu \, v_l \, \varepsilon_Z^\mu = \bar{u}_l \, \gamma_\mu \left(g_v + g_a \, \gamma_5 \right) v_l \, \varepsilon_Z^\mu, \qquad s = M_Z^2. \qquad (44)$$

Therefore g_v and g_a can be obtained from the matrix $\mathcal{M}^\mu$ by using suitable projectors:

$$\frac{1}{D} \, \text{Tr} \left(\gamma_\mu \, \mathcal{M}^\mu \right), \qquad g_a = -\frac{1}{D} \, \text{Tr} \left(\gamma_\mu \, \gamma_5 \, \mathcal{M}^\mu \right), \qquad (45)$$

where D is the dimension of the space-time. Among the electroweak two-loop diagrams contributing to $\mathcal{M}^\mu$, we started considering those containing a closed fermion loop (this computation has been recently done by Awramik, Czakon, Freitas and Weiglein in [12]). They are represented in Fig. 3.

We started applying our methods on configuration c which is the most difficult one. The strategy used is the following:

- Write the amplitude, considering the different contributions to configuration c. This generates a sum of tensor integral of the family V^{231}.
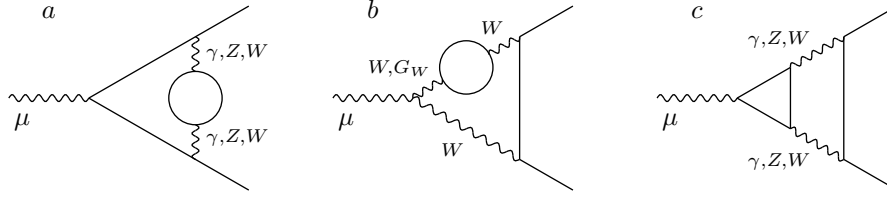
Fig. 3. Diagrams contributing to the fermionic corrections to $\sin^2 \theta_{\text{eff}}^{\text{lept}}$. Because of CP conservation, diagrams involving the Higgs boson cancel and are not included.

- Perform a simple reduction of tensor integral of the following type:

$$\frac{2\,q \cdot p}{(q^2 + m^2)[(q+p)^2 + M^2]}$$
$$= \frac{1}{q^2 + m^2} - \frac{1}{(q+p)^2 + M^2} - \frac{p^2 - m^2 + M^2}{(q^2 + m^2)[(q+p)^2 + M^2]} \cdot (46)$$

This kind of reduction does not introduce any new denominator and therefore any spurious singularity. At this point we have a sum of scalar and vector integrals belonging to 4 vertex families (V^{121}, V^{131}, V^{221} and V^{231}), together with some self-energies and some one-loop diagrams.

- Combine the sum of all these diagrams in just *one* integral.

Just to show the efficiency of the numerical computation, we give some preliminary results. We consider the expansion in loops for g_v/g_a

$$g_{v,a} = g_{v,a}^0 + g_{v,a}^1 + g_{v,a}^2 \,, \tag{47}$$

$$\frac{g_v}{g_a} = \frac{g_v^0}{g_a^0} \left[1 + \frac{g_v^1}{g_v^0} - \frac{g_a^1}{g_a^0} - \frac{g_a^1}{g_a^0} \left(\frac{g_v^1}{g_v^0} - \frac{g_a^1}{g_a^0} \right) + \frac{g_v^2}{g_v^0} - \frac{g_a^2}{g_a^0} \right] , \tag{48}$$

where the last two terms represent the pure two-loop corrections to $\sin^2 \theta_{\text{eff}}^{\text{lept}}$. The contribution to these corrections coming from diagram c (Fig. 3) with two Z or two W is:

$$\left(\frac{g_v^2}{g_v^0} - \frac{g_a^2}{g_a^0} \right)_{ZZ} = -0.279937 \times 10^{-5} \pm 0.15 \times 10^{-9},$$

$$\left(\frac{g_v^2}{g_v^0} - \frac{g_a^2}{g_a^0} \right)_{WW} = 0.577269 \times 10^{-1} \pm 0.14 \times 10^{-5}. \tag{49}$$

In this result the contributions coming from all possible fermion loops are summed up. In particular it includes the diagrams containing the top quark

which in the usual analytical approach require an expansion in the ratio $M_Z/m_t \sim 1/4$.

8. Conclusions

The techniques described in this paper show that the numerical approach to Feynman integrals allows the computation of diagrams that cannot be treated within the usual analytical approach. Under this point of view, would be interesting to apply these methods, and in particular the new one, to more complicated two-loop diagrams (the two-loop 4-point functions for example). In addition to that, the first results obtained from the application of these techniques to the fermionic correction to $\sin^2 \theta_{\rm eff}^{\rm lept}$, seem to show that the numerical approach is not only suited for the computation of single integrals, but can also be applied to the complete evaluation of physical observables (which requires to sum up several diagrams). Of course the computation must be completed to give a serious proof of that.
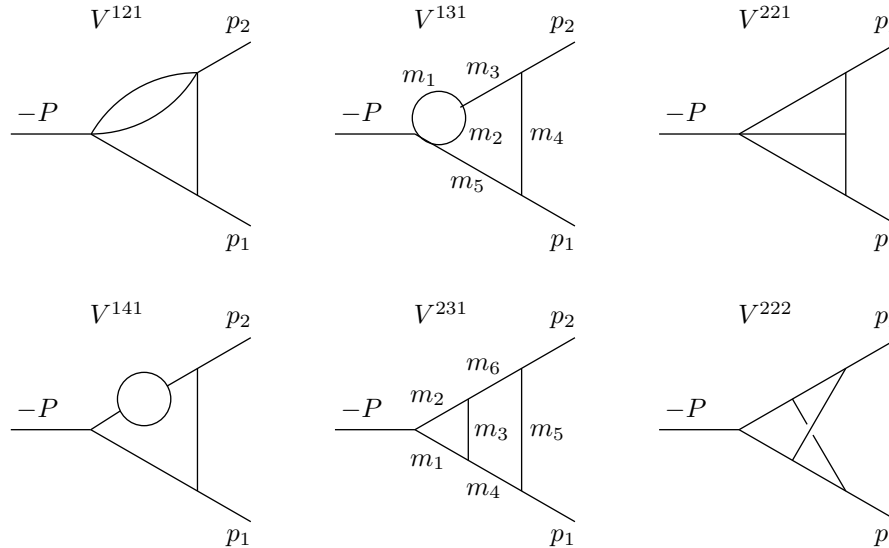
Appendix A

Fig. 4. Two-loop vertex topologies. The momenta are all incoming.

REFERENCES

[1] [LEP Collaboration], hep-ex/0312023.

[2] A.I. Davydychev, V.A. Smirnov, *Nucl. Instrum. Methods* **A502**, 621 (2003).

[3] R. Bonciani, P. Mastrolia, E. Remiddi, *Nucl. Phys.* **B661**, 289 (2003).

[4] F.V. Tkachov, *Nucl. Instrum. Methods* **A389**, 309 (1997); L.N. Bertstein, *Functional Analysis and its Applications* **6**, 66 (1972).

[5] G. Passarino, *Nucl. Phys.* **B619**, 257 (2001).

[6] G. Passarino, S. Uccirati, *Nucl. Phys.* **B629**, 97 (2002).

[7] A. Ferroglia, M. Passera, G. Passarino, S. Uccirati, *Nucl. Phys.* **B650**, 162 (2003).

[8] A. Ferroglia, G. Passarino, M. Passera, S. Uccirati, Prepared for 31st International Conference on High Energy Physics (ICHEP 2002), Amsterdam, The Netherlans; A. Ferroglia, G. Passarino, S. Uccirati, M. Passera, *Nucl. Instrum. Methods* **A502**, 391 (2003).

[9] A. Ferroglia, M. Passera, G. Passarino, S. Uccirati, *Nucl. Phys.* **B680**, 199 (2004).

[10] S. Actis, A. Ferroglia, G. Passarino, M. Passera, S. Uccirati, hep-ph/0402132.

[11] R. Erdelyi *et al.*, *Higher Transcendental Functions*, vol. 2, Bateman Manuscript Project, McGraw-Hill, 1953; L.J. Slater, *Generalized Hypergeometric Functions*, Cambridge Univ. Press, 1966.

[12] M. Awramik, M. Czakon, A. Freitas, G. Weiglein, hep-ph/0407317.